A Sequential 3D Thinning Algorithm and Its Medical Applications

Kálmán Palágyi[1], Erich Sorantin[2], Emese Balogh[1], Attila Kuba[1], Csongor Halmai[1], Balázs Erdőhelyi[1], and Klaus Hausegger[2]

[1] Department of Applied Informatics, University of Szeged, Hungary
{palagyi, bmse, kuba, halmai}@inf.u-szeged.hu
[2] Department of Radiology, University Hospital Graz, Austria
{erich.sorantin, klaus.hausegger}@kfunigraz.ac.at

Abstract. Skeleton is a frequently applied shape feature to represent the general form of an object. Thinning is an iterative object reduction technique for producing a reasonable approximation to the skeleton in a topology preserving way. This paper describes a sequential 3D thinning algorithm for extracting medial lines of objects in $(26,6)$ pictures. Our algorithm has been successfully applied in medical image analysis. Three of the emerged applications (analysing airways, blood vessels, and colons) are also presented.

1 Basic Notions and Results

Let p be a point in the 3D digital space $\mathbb{Z}^3$. Let us denote $N_j(p)$ (for $j = 6, 18, 26$) the set of points *j–adjacent* to point p (see Fig. 1/a). The sequence of distinct points $\langle x_0, x_1, \ldots, x_n \rangle$ is a *j–path* of length $n \geq 0$ from point x_0 to point x_n in a non–empty set of points X if each point of the sequence is in X and x_i is j–adjacent to x_{i-1} for each $1 \leq i \leq n$. (Note that a single point is a j–path of length 0.) Two points are *j–connected* in the set X if there is a j–path in X between them. A set of points X is *j–connected* in the set of points $Y \supseteq X$ if any two points in X are j–connected in Y.

The *3D binary (m,n) digital picture* $\mathcal{P}$ is a quadruple $\mathcal{P} = (\mathbb{Z}^3, m, n, B)$ [2]. Each element of $\mathbb{Z}^3$ is called a *point* of $\mathcal{P}$. Each point in $B \subseteq \mathbb{Z}^3$ is called a *black point* and value 1 is assigned to it. Each point in $\mathbb{Z}^3 \backslash B$ is called a *white point* and value 0 is assigned to it. Adjacency m belongs to the black points and adjacency n belongs to the white points. A *black component* (or *object*) is a maximal m–connected set of points in B. A *white component* is a maximal n–connected set of points in $B \subseteq \mathbb{Z}^3$. We are dealing with (26,6) pictures. It is assumed that any picture contains finitely many black points.

A black point in a $(26,6)$ picture is called *border point* if it is 6–adjacent to at least one white point. A border point p is called U–*border point* if the point marked by "U" in Fig. 1/a is white. We can define N–, E–, S–, W–, and D–border points in the same way. A black point is called *end–point* if it has exactly one black 26–neighbor (i.e., the set $N_{26}(p) \cap (B \backslash \{p\})$ is singleton).

M.F. Insana, R.M. Leahy (Eds.): IPMI 2001, LNCS 2082, pp. 409–415, 2001.

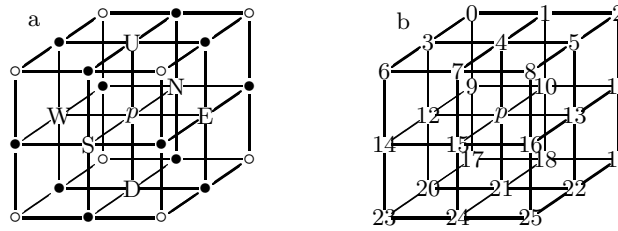

Fig. 1. (a) The frequently used adjacencies in $\mathbb{Z}^3$. The set $N_6(p)$ contains the central point p and the 6 points marked U, N, E, S, W, and D. The set $N_{18}(p)$ contains the set $N_6(p)$ and the 12 points marked "•". The set $N_{26}(p)$ contains the set $N_{18}(p)$ and the 8 points marked "○". (b) Indices assigned to points in $N_{26}(p)\backslash\{p\}$

A black point is called *simple point* if its deletion does not alter the topology of the picture. We make use of the following result for (26,6) pictures:

Theorem 1. [4] *Black point p is simple in picture $(\mathbb{Z}^3, 26, 6, B)$ if and only if all the following conditions hold:*

1. *the set $N_{26}(p) \cap (B\backslash\{p\})$ is not empty (i.e., p is not an isolated point);*
2. *the set $N_{26}(p) \cap (B\backslash\{p\})$ is 26–connected (in itself);*
3. *the set $(\mathbb{Z}^3\backslash B) \cap N_6(p)$ is not empty (i.e., p is a border point); and*
4. *the set $(\mathbb{Z}^3\backslash B) \cap N_6(p)$ is 6–connected in the set $(\mathbb{Z}^3\backslash B) \cap N_{18}(p)$.*

2 Skeletonization by Thinning

The notion of *skeleton* was introduced by Blum [1] as a region–based shape descriptor which summarises the general form of objects/shapes. The thinning is a frequently used method for producing an approximation to the skeleton in a topology–preserving way [2]. Border points of a binary object that satisfy certain topological and geometric constraints are deleted in iteration steps. The entire process is repeated until only the "skeleton" is left. In case of "near tubular" 3D objects (e.g., airway, blood vessel, and gastro–intestinal tract), Thinning has a major advantage over the other skeletonization methods since *curve thinning* can produces *medial lines* easily [5].

Most of the existing thinning algorithms are parallel, but some sequential thinning algorithms have been proposed [6,7] and there is a hybrid one (i.e., deletable points are marked in parallel then a sequential re–checking phase is needed) [3]. This paper presents an effective sequential 3D thinning algorithm for extracting medial lines from elongated binary objects.

3 The New 3D Thinning Algorithm

Let $(\mathbb{Z}^3, 26, 6, B)$ be a 3D finite picture to be processed. Since set B is finite, it can be stored in a finite 3D binary array X (each voxel being not in X is looked on 0).

The pseudocode of the sequential 3D thinning algorithm is given as follows:

```
procedure THINNING(X,Y)
Y = X;
repeat
    modified = 0;
    modified = modified+SUBITER(Y,U);
    modified = modified+SUBITER(Y,D);
    modified = modified+SUBITER(Y,N);
    modified = modified+SUBITER(Y,S);
    modified = modified+SUBITER(Y,E);
    modified = modified+SUBITER(Y,W);
until  modified > 0;
```

```
function SUBITER ( Y, direction )
modified = 0;
list =< new empty list >;
for each point p in Y do
    if IS_BORDER_POINT(Y,direction,p) then
        Np = COLLECT_26_NEIGHBORS ( Y, p );
        if not IS_ENDPOINT ( Np ) then
            if IS_SIMPLE ( Np ) then
                INSERT_LIST ( list , p );
while IS_EMPTY ( list ) do
    p = GET_FROM_LIST ( list );
    Np = COLLECT_26_NEIGHBORS ( p , Y );
    if not IS_ENDPOINT ( Np ) then
        if IS_SIMPLE ( Np ) then
            SET_ZERO ( Y , p );
            modified = modified +1;
return modified;
```

The two parameters of the procedure THINNING are the binary array X representing the picture to be thinned and the binary array Y storing the result. The kernel of the **repeat** cycle corresponds to one iteration step of the thinning process. Each iteration step is composed of six successive subiterations corresponding to the six kinds of border points. Some U–border points can be deleted in the first subiteration and certain W–border points are deleted in the sixth one. In this way, the elongated objects are shrunk uniformly in each direction. Function SUBITER returns the number of deleted points. Variable *modified* is to accumulate the number of deleted points. The thinning process is completed when no points are deleted (i.e., no further changes occur).

The work of function SUBITER is composed of two phases. All the border points of a given type being simple and non–end–points are inserted in a linked list called *list* in the first phase (see the **for** cycle). This phase (i.e., marking points for deletion) is followed by a sequential re–checking procedure (see the **while** cycle): each point in the list is removed if it remains simple and non–end–points in the actual (modified) image. Function SUBITER uses an additional auxiliary data structure: Np is an array of 26 binary digits. Function COLLECT_26_NEIGHBORS returns such an array storing the 26–neighbors of an investigated point p in an image array Y, where $Np[i]$ corresponds to the neighbor marked "i" in Fig. 1/b ($i = 0, \ldots, 25$). Since both the simplicity and being end–point are local properties, they can be decided in view of array Np. These properties are answered by functions IS_SIMPLE and IS_ENDPOINT, respectively. Function IS_ENDPOINT returns NO if $\sum_{i=0}^{25} Np[i] > 1$. (Note that an isolated point is regarded as an end–point by this function.)

Function IS_SIMPLE is to check the second and the fourth conditions of Theorem 1. The first and the third conditions of Theorem 1 are satisfied, since function IS_ENDPOINT returns YES if the investigated point p is isolated and p is always border point of the given type when function IS_SIMPLE is called. Function IS_COND_2_SATISFIED uses two auxiliary data structures: The first one is the array L of 26 integers, where $L[i]$ stores a label assigned to the element represented by $Np[i]$ $(i = 0, \ldots, 25)$. The second one is the key to the labelling process: $S26$ is an array of 26 sets of indices, where

$$S26[i] = \{\ j \mid j \in N_{26}(i) \text{ and } 0 \leq j < i\ \} \quad (i = 0, \ldots, 25).$$

For example: $S26[0] = \emptyset$, $S26[1] = \{0\}$, and $S26[25] = \{13, 15, 16, 21, 22, 24\}$ (see Fig. 1/b).

All the sets $S26[0], \ldots, S26[25]$ can be stored (for example) in explicit arrays. It is easy to see that the black 26–neighbors (stored in the array Np) of a point p is 26–connected if the same label belongs to each black 26–neighbors of p. Note that the function IS_COND_4_SATISFIED applies a similar labelling procedure. Let us see the remaining two important functions.

```
function IS_SIMPLE ( Np )
if IS_COND_2_SATISFIED ( Np ) then
    if IS_COND_4_SATISFIED ( Np ) then
        return YES;
return NO;
```

```
function IS_COND_2_SATISFIED ( Np )
label = 0;
for i = 0 to 25 do
    L[i] = 0;
for i = 0 to 25 do
    if Np[i] = 1 then
        label = label +1;
    for each j in S26[i] do
        if L[j] > 0 then
            for k = 0 to i − 1 do
                if L[k] = L[j] then L[k] = label;
for i = 0 to 25 do
    if Np[i] = 1 and L[i] ≠ label then
        return NO;
return YES;
```

4 Applications

This section is devoted to the emerged applications applying our sequential 3D thinning algorithm.

Each of the following three applications requires the cross–sectional profiles of the investigated tubular organs. The proposed process is sketched as follows:

- image acquisition by Spiral Computed Tomography (S–CT),
- (semiautomatic snake–based) segmentation (i.e., determining a binary object from the gray–level picture,
- morphological filtering of the segmented object,
- curve thinning (by using our 3D thinning algorithm),
- raster–to–vector conversion,
- pruning the vector structure (i.e., removing the unwanted branches),
- smoothing the resulted *central path*,
- calculation of the *cross–sectional profile* orthogonal to the central path.

4.1 Assessment of Laryngotracheal Stenosis

Many conditions can lead to laryngotracheal stenosis (LTS), most frequent endotracheal intubation, followed by external trauma, or prior airway surgery. Clinical management of these stenosis requires exact information about the number, grade, and the length of the stenosis. We have developed a method for assessment of LTS. The cross–sectional profiles (based on the central path) of the upper respiratory tract (URT) were calculated for 30 patients with proven LST on fiberoptic endoscopy (FE). Locations of LTS were determined on axial S–CT slices and compared to findings of fiberoptic endoscopy (FE) by Cohen's kappa statistics. Regarding the site of LTS an excellent correlation was found between FE and S–CT ($z = 7.44$, $p < 0.005$). Site of LTS, length and degree could be depicted on the URT cross-sectional charts in all patients.

URT cross sectional profiles were presented as line charts. In order to establish anatomic cross-reference, three important anatomic landmarks (vocal cords, caudal border of the cricoid cartilage, and cranial border of the sternum) were marked on the line charts (see Fig. 2). For validation of this method, 13 phantom studies were performed. Phantom studies yielded an error of 1% for length measurements and an excellent correlation was found between the theoretical cross-sectional profile of phantoms and that obtained by our thinning algorithm ($p \ll 0.005$).

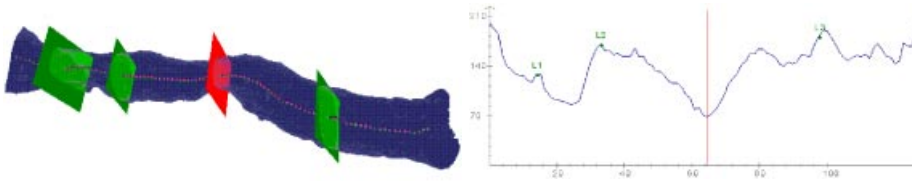

Fig. 2. The segmented URT, its central paths, its cross–sectional profile at the three landmarks, and at the narrowest position (left) and the line chart (right)

4.2 Assessment of Infrarenal Aortic Aneurysms

We used the cross–sectional profile in patients suffering from infra–renal aortic aneurysms (AAA). AAA are abnormal dilatations of the main arterial abdominal vessel due to atherosclerosis. AAA can be found in 2% of people older than 60 years. If the diameter is more than 5 cm than the person is at high risk for AAA rupture, which leads to death in 70–90%. For therapy two main options exist: surgery or endoluminal repair with stentgrafts. For optimal patient management the "true diameter" in 3D as well as the distance to the origin of the renal arteries (proximal aneurysma neck) as well as the extension to the iliac arteries (distal aneurysma neck) have to be known.

The same algorithm as for LTS was applied. Using an active contour model the abdominal aorta was segmented, followed by the thinning process and computation of the cross sectional profile. Results were again presented as line charts. Figure 3 shows the segmented infrarenal aorta and its central path. Along the central path the cross–sectional profile was computed. The following parameters could be derived from this approach: the maximum diameter in 3D as well as the length of the proximal and distal neck of the aneurysma. Since size of the aneurysma is regarded to be a prognostic factor, the volume of the segmented aneurysma was determined too. At follow–up investigations the same parameters were derived.

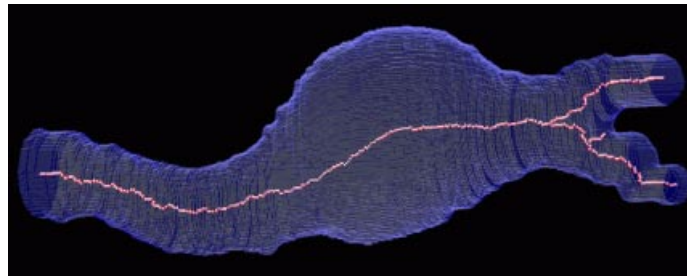

Fig. 3. The segmented part of the blood vessel and its central path

Insertion of stent grafts could be planned easily using this charts. At follow-up investigations in the regular case the volume of the infrarenal aneurysms declined, whereas in the others leakage could be detected in a high proportion.

4.3 Unravelling the Colon

Unravelling the colon is a new method to visualize the entire inner surface of the colon without the need for navigation. This is a minimally invasive technique that can be used for colorectal polyps and cancer detection. In this section we present an algorithm for unravelling the colon which is to digitally straighten and then flatten using reconstructed spiral/helical computer tomograph (CT) images. Comparing to virtual colonoscopy where polyps may be hidden from view behind the folds, the unravelled colon is more suitable for polyp detection, because the entire inner surface is displayed at one view.

To test the algorithm we used a cadavric phantom, a 50 cm long cadavric colon. The colon was cleansed and 13 artificial polyps were created using fat tissues. After air insufflation the specimen was placed in a 5 l water bath containing 5 ml Gastrografin solution. The phantom was scanned using multirow detector CT using a collimation of 2.5 mm, and a high quality pitch. Images were reconstructed with a slice thickness of 1.25 mm and an increment of 0.5 mm. Altogether 750 CT slices were reconstructed. The results were compared to the real dissection of the phantom.

After calculating the cross–sectional profile the segmented colon is remapped (into a new grey–level 3D data volume) and displayed.

Because of the tortuous structure of the colon nearby cross sections may conflict and as a result polyps may be missed or counted multiple times. To avoid this we interpolate and recalculate iteratively the cross sections till we resolve the conflict. This results that the internal and external colon surfaces are slightly stretched or compressed. The last step is to display the straightened and flattened colon using surface rendering.

The simulated polyps can be recognized, they appeared as bumps or as asymmetric broadening of the colon folds (see Fig. 4).

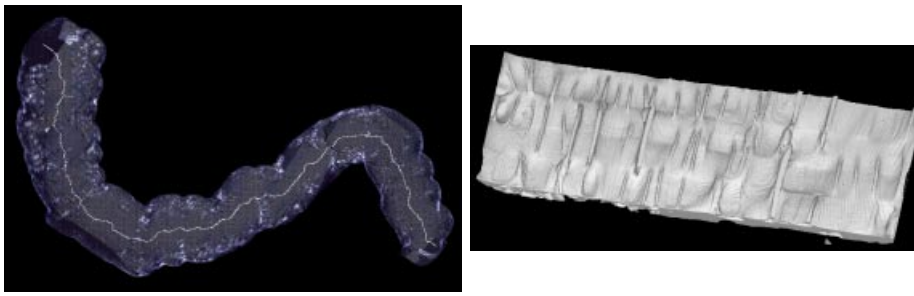

Fig. 4. The segmented volume of the cadavric phantom and its central path (left) and the unravelled colon (right)

Acknowledgment

This work was supported by the CEEPUS A-34 and FKFP 0908/1997 Grants.

References

1. Blum, H.: A transformation for extracting new descriptors of shape. Models for the Perception of Speech and Visual Form, MIT Press, (1967) 362–380
2. Kong, T.Y., Rosenfeld, A.: Digital topology: Introduction and survey. Computer Vision, Graphics, and Image Processing **48** (1989) 357–393
3. Lee, T., Kashyap, R.L., Chu, C.: Building skeleton models via 3–D medial surface/axis thinning algorithms. CVGIP: Graphical Models and Image Processing **56** (1994) 462–478
4. Malandain, G., Bertrand, G.: Fast characterization of 3D simple points. In: Proc. 11th IEEE International Conference on Pattern Recognition (1992) 232–235
5. Palágyi, K., Kuba, A.: A parallel 3D 12–subiteration thinning algorithm. Graphical Models and Image Processing **61** (1999) 199–221
6. Saha, P.K., Chaudhuri, B.B.: Detection of 3–D simple points for topology preserving transformations with application to thinning. IEEE Transactions on Pattern Analysis and Machine Intelligence **16** (1994) 1028–1032
7. Saito, T., Toriwaki, J.: A sequential thinning algorithm for three dimensional digital pictures using the Euclidean distance transformation. In: Proc. 9th Scandinavian Conf. on Image Analysis, SCIA'95 (1995) 507–516